THE JOURNAL OF PHYSICAL CHEMISTRY B

ARTICLE

pubs.acs.org/JPCB

The Impact of Texas Red on Lipid Bilayer Properties

Michael J. Skaug, Marjorie L. Longo, and Roland Faller*

Department of Chemical Engineering and Materials Science, University of California—Davis, Davis, California 95616, United States

ABSTRACT: We investigated the impact of fluorescent labeling on the properties of a lipid bilayer using atomistic molecular dynamics simulation. The system consisted of 24 Texas Red−1,2-dihexadecanoyl-*sn*-glycero-3-phophoethanolamine (TR−DHPE) in a bilayer of 488 1,2-dipalmitoyl-*sn*-glycero-3-phosphocholine (DPPC) lipids. We found binding between TR−DHPE and DPPC caused by electrostatic interactions. On average, TR−DHPE is bound to 1.2 DPPC molecules. Binding reduced the diffusion coefficient of TR−DHPE by 34% relative to unlabeled DPPC molecules. We estimate that binding would lead to a ∼ 5 °C increase in the liquid to liquid-ordered transition temperature of a ternary lipid system. These results emphasize the importance of considering the impact of fluorescence labeling when interpreting experimental results.

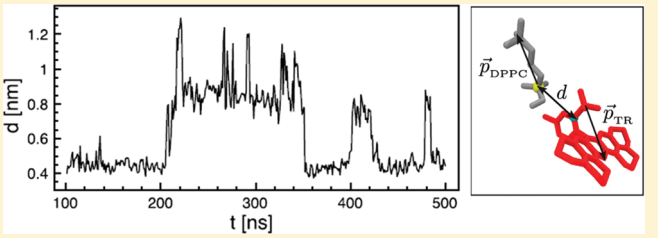

INTRODUCTION

Fluorescent molecules are commonly used experimental tools to study lipid membrane structure and dynamics. There is a wide range of synthetic fluorophores available which are either covalently linked to a lipid or naturally partition into the hydrophobic membrane core. When introduced at a relatively low concentration (<5 mol %), these fluorescent impurities allow a variety of optical techniques to be applied, such as microscopy,[1] fluorescence correlation spectroscopy (FCS),[2] fluorescence resonance energy transfer (FRET),[3] and single molecule tracking (SMT).[4] The implicit assumption in every fluorescence experiment is that the fluorophore does not alter the properties of the lipid membrane. A variety of experiments have cast doubt on this assumption. Veatch et al. found that even very small concentrations (∼0.2 mol %) of a fluorescent dye could increase the mixing transition temperature of a ternary lipid system by 5 °C.[5] Similar increases in transition temperature were found for a variety of fluorophores in a systematic study by Juhasz et al.[6] Bouvrais et al. investigated the mechanical properties of lipid bilayers containing several fluorophores and found that some produced a reproducible change in the membrane bending elasticity.[7] The impact of fluorescent labeling on dynamics was discovered by Daniel et al., who were spreading a negatively charged fluorophore using lipid bilayer electrophoresis and found two dynamic populations caused by two isomers of the fluorophore.[8]

In light of these experimental findings, it is important to consider the possible impact of fluorescent labeling on lipid bilayer properties. One of the most commonly used fluorophores in lipid membrane studies is Texas Red−DHPE.[9−11] Texas Red, or sulforhodamine 101 acid chloride, is a polycyclic aromatic with a molecular weight of 652.2 g/mol.[12] When covalently linked to the headgroup of DHPE, the complete molecule has a net −1e charge and partitions into the disordered phase of lipid bilayers.[13] Being negatively charged and twice the mass DPPC, it seems quite possible that TR−DHPE would behave differently and influence the properties of a lipid membrane.

Our goal is to determine what influence Texas Red−DHPE has on the properties of a lipid bilayer. For this purpose, we used atomistic molecular dynamics which allowed us to analyze the behavior of TR−DHPE and unlabeled DPPC in the same system. The atomistic resolution of the simulations also allowed us to determine the molecular origin of any Texas Red influence on the bilayer. Molecular dynamics simulations have been used to study lipid bilayers labeled with other fluorophores, including the free hydrophobic probes diphenylhexatriene[14−16] and pyrene,[17,18] tail labeled probes NBD-PC[19,20] and pyrene−PC,[21] and DiI−C18.[22] Of these, only DiI−C18 has a net charge and none are of the commonly used class of headgroup labeled probes. Texas Red−DHPE is negatively charged and is representative of the headgroup labeled class of bilayer probes. In this article, we present results which illustrate the impact of Texas Red−DHPE on the dynamics and phase behavior of a lipid bilayer, and we suggest a mechanism for results seen experimentally.

SIMULATION METHODS

All molecular dynamics simulations were performed using Gromacs 4.0.4, keeping the number of particles, temperature and pressure constant.[23−25] The force field parameters for 1,2-dipalmitoyl-*sn*-glycero-3-phosphocholine (DPPC) were developed by Berger et al.[26] and have been thoroughly validated.[23] The force field parameters for Texas Red−1,2-dihexadecanoyl-*sn*-glycero-3-phophoethanolamine (TR−DHPE) were previously developed and validated.[27] TR−DHPE has the same lipid structure as DPPE, but conforms to the IUPAC naming convention. The chemical structure of DPPC and the Texas Red portion of TR−DHPE are shown in Figure 1. The simulated system was based on a 512 DPPC bilayer. We chose a DPPC bilayer because TR−DHPE is a fluid phase probe and fluid phase DPPC has

Received: April 21, 2011
Revised: June 4, 2011
Published: June 06, 2011

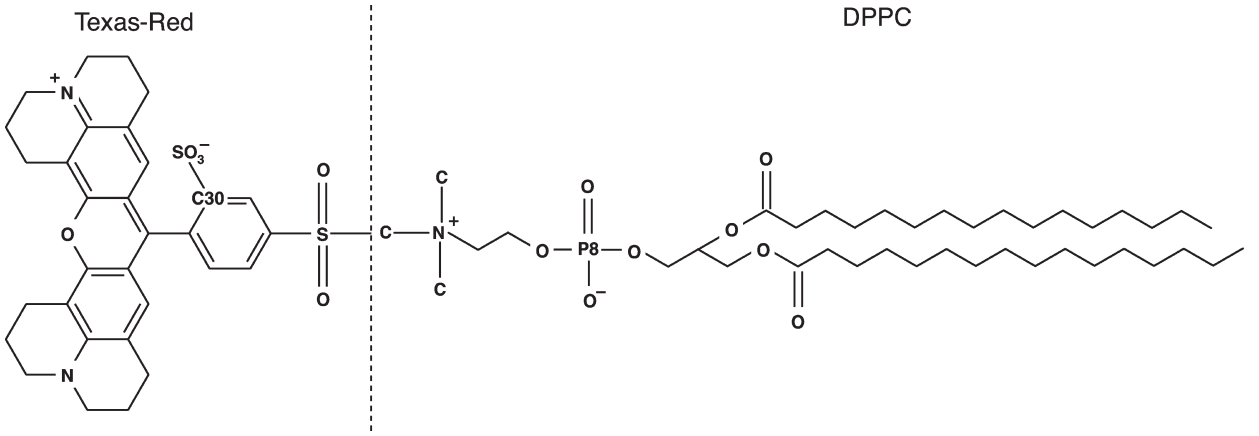

Figure 1. Chemical structures of Texas Red and DPPC molecules. TR−DHPE is produced by bonding the Texas Red to the DPPC headgroup, except that the choline is replaced with an ethanolamine. Two atoms have been specifically labeled as C30 and P8 for reference later in the paper.

been extensively studied using molecular dynamics. In the simulated system, 24 DPPC molecules were replaced with TR−DHPE molecules resulting in a Texas Red concentration of 4.7 mol %. We used this concentration, which is on the high end of experimental Texas Red concentrations, to maximize the statistics for TR−DHPE. The composition was symmetric between the two bilayer leaflets. The bilayer was solvated with 26.5 SPC[28] waters per lipid and 24 Na^+ ions to neutralize the −1e charge on each of the TR−DHPE molecules. The sodium interaction parameters were taken from the Gromos 87 force−field.[29] The temperature of the system was weakly coupled to an external 325 K bath using a Berendsen thermostat with a time constant of 0.2 ps.[30] The pressure was maintained constant at 1 bar in each of the three directions independently to allow equilibration of the bilayer area. Again, the Berendsen weak−coupling algorithm with a time constant of 2.0 ps was used to control the pressure. The system was simulated with a time step of 2 fs and the LINCS algorithm was used to constrain all DPPC and TR−DHPE bond lengths.[31] The SPC water bond lengths were constrained using the SETTLE algorithm.[32] Electrostatics were treated with the PME method and a coulomb cutoff of 1.2 nm.[33] van der Waals interactions were switched over the distance 0.8 to 1.0 nm and shifted so they decayed to zero at 1.0 nm. The neighbor list of each particle was cutoff at 1.2 nm and updated every 10 steps. Periodic boundaries were applied in all three directions. The system was simulated for 500 ns. The system was still equilibrating during the first 100 ns, so only the last 400 ns were used in the following analysis.

RESULTS AND DISCUSSION

Binding of Texas Red and DPPC. Previous work[27] suggested that Texas Red might bind to DPPC molecules in a fluid bilayer. With a longer simulation and a greater number of TR−DHPE, we are now able to quantitatively describe the binding between Texas Red and unlabeled DPPC molecules. The binding occurs between the phosphate group of a DPPC and the aryl group of the TR−DHPE. Therefore, we use the distance (d) between the DPPC phosphorus atom (P8) and the carbon atom bonded to the SO_3 group (C30), as the order parameter of binding. Figure 2b is an example of this distance over the last 400 ns of the simulation. In contrast, Figure 2a is the interphosphorus

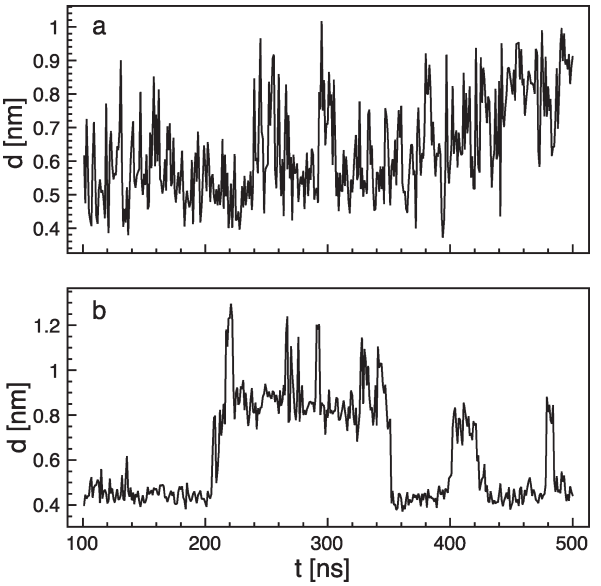

Figure 2. (a) Time evolution of the distance between two neighboring DPPC phosphorus atoms, illustrating the typical intermolecular distance fluctuations observed. (b) Time evolution of the separation between a TR and a bound DPPC clearly showing multiple binding events and suppressed fluctuations at the lowest separation.

distance between two neighboring DPPC molecules, illustrating the typical fluctuations observed.

In order to quantify the residence time and number of DPPC bound, we define the bound state to be a Texas Red−DPPC pair with a C30−P8 separation distance d < 0.7 nm. Figure 3 is a distribution of the residence time for the Texas Red−DPPC bound state and we see that the distribution is very long tailed (notice the log scale on the horizontal axis). The average residence time is 17 ns, but there are some that remain bound for the entirety of the 500 ns simulation.

We also find that TR−DHPE is frequently bound to two DPPC molecules and occasionally even three (Inset of Figure 3). On average, TR−DHPE is bound to 1.2 DPPC molecules. On the basis of careful inspection of the trajectory and distance plots like Figure 2, we believe there are at least two unique binding locations for DPPC on the Texas Red. It was previously shown[27]

dx.doi.org/10.1021/jp203738m |J. Phys. Chem. B 2011, 115, 8500–8505

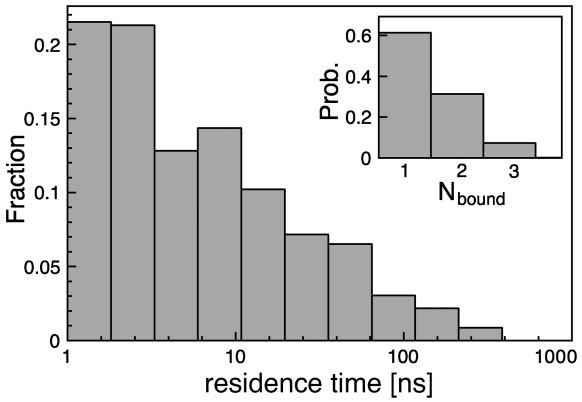

Figure 3. Distribution of residence time for binding events between Texas Red and DPPC. (Inset) The probability for the number of DPPC bound to a Texas Red at one time, N_{bound}.

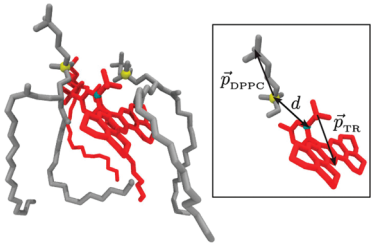

Figure 4. A snapshot of the typical configuration of TR−DHPE and two bound DPPC molecules. The P8 phosphorus atom of the DPPC is shown in yellow and the C30 carbon atom of TR−DHPE is shown in cyan. (Inset) Definition of the TR−DHPE and DPPC molecular dipoles, $\vec{p}_{TR}$ and $\vec{p}_{DPPC}$ and the TR−DHPE−DPPC distance d.

that TR−DHPE adopts a bent configuration in the fluid bilayer, with the lipid tails and the Texas Red xanthene structure positioned in the hydrophobic core of the bilayer. This allows the more highly charged, phosphate and sulfur groups to remain near the interphase. The most closely bound DPPC locates in the bend of TR−DHPE, between the lipid and xanthene sections of TR−DHPE. As a result, the closest contact is between the bound DPPC phosphate group and the aryl ring of the Texas Red, with an average separation of about 0.4 nm. The frequently observed second bound DPPC is located on the outside face of the Texas Red xanthene and has an average bound separation of about 0.6 nm. A snapshot of the typical configuration is shown in Figure 4. These two bound states may be reflected in the residence time distribution of Figure 3, where we observe a peak near 2 ns and another near 10 ns.

The two binding locations can also be identified in the radial distribution function between the TR−DHPE C30 atoms and the DPPC phosphorus atoms. Figure 5 shows the large first peak in the C30−P8 radial distribution function due to binding, whose asymmetry may be due to the two slightly different binding distances. To get an idea of the strength of the binding, we can use the radial distribution function to estimate the potential of mean force using the following expression,

$$w(r) = -k_b T \ln(g(r)) \quad (1)$$

The calculated potentials of mean force are displayed in the inset of Figure 5 and demonstrate that the TR−DHPE−DPPC interaction has a minimum deeper than 1 kT, indicative of binding,

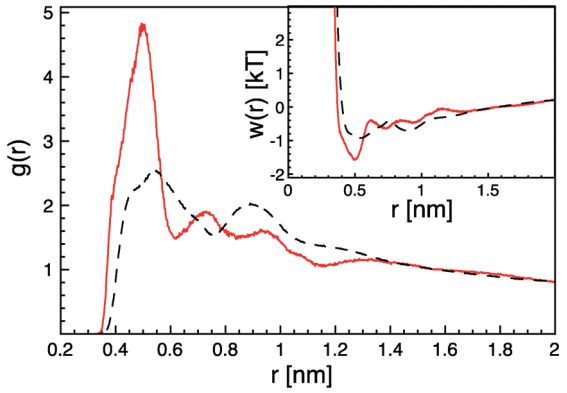

Figure 5. Radial distribution function between TR−DHPE C30 and DPPC phosphorus (solid red). For comparison, the dashed black line is the radial distribution function between DPPC phosphorus. (Inset) Corresponding potentials of mean force derived from the radial distribution functions using eq 1.

whereas the DPPC−DPPC interaction is not strong enough to cause binding.

The Cause of Binding. The binding of TR−DHPE and DPPC occurs between highly polar and charged regions of each molecule, which suggests an electrostatic interaction as the source of binding. Texas Red has a net charge of −1e, whereas DPPC is neutral with a net dipole moment in its headgroup. Therefore, the two leading terms in the TR−DHPE−DPPC electrostatic interaction are charge−dipole and dipole−dipole. To investigate this further, we looked at the behavior of the TR−DHPE and DPPC molecular dipoles. In the following analysis, we present the average behavior of all bound DPPC molecules rather than separate the different bound states. We believe that the cause of binding is the same for each state, so we expect their behaviors to be similar. For DPPC, the net dipole moment roughly points from the phosphorus to the choline nitrogen and has a magnitude of 17.3 D. Because TR−DHPE has a net charge, the dipole moment depends on the choice of origin. On the basis of convention, we took the Texas Red center of mass as the origin and found a net dipole moment of magnitude 21.1 debye that points roughly from the sulfonate sulfur to the xanthene oxygen. The definition of the Texas Red and DPPC molecular dipoles are shown in the inset of Figure 4. In Figure 6a, we see that on average, the Texas Red dipole is in an attractive configuration with the bound DPPC dipole, $\theta_{dip-dip} = 113 \pm 29°$. The angle distribution for unbound pairs is broader, more symmetric and less attractive. We also find that the DPPC dipoles tilt more toward the bilayer normal when bound to TR−DHPE (Figure 6b), presumably to adopt a more attractive orientation with the Texas Red dipole.

Not only does the DPPC dipole orientation change when bound, its dynamics also changes. We calculated the rotational autocorrelation of bound and unbound DPPC molecular dipoles using the expression

$$C(t) = \langle \cos \theta \rangle \quad (2)$$

where θ is the angle between the dipole at times τ and $\tau + t$. Figure 7 demonstrates that the dipoles of bound DPPC reorient much more slowly than those of unbound DPPC. Fitting each of the autocorrelations with a single exponential, we find the bound

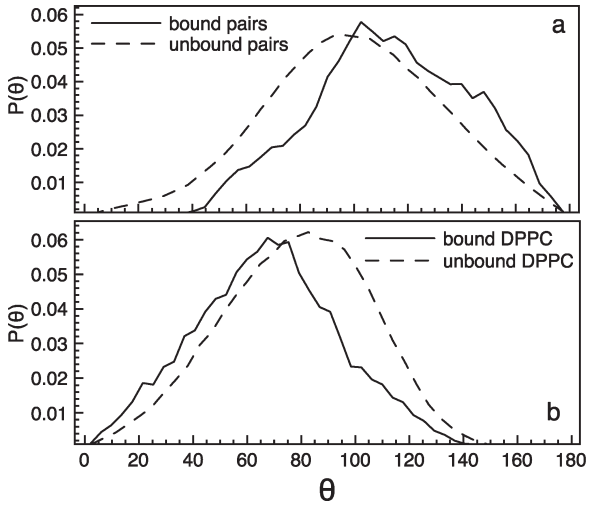

Figure 6. (a) Distribution of the angle between the molecular dipoles of bound (solid) and unbound (dashed) DPPC−TR−DHPE pairs. (b) Distribution of the angle between the bound (solid) and unbound (dashed) DPPC molecular dipoles and the simulation z direction.

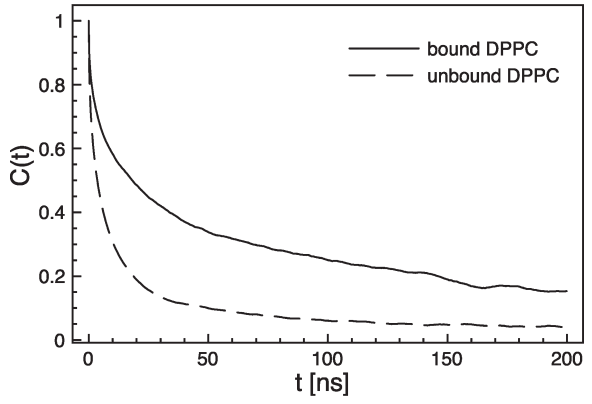

Figure 7. Rotational autocorrelation of bound (solid) and unbound (dashed) DPPC molecular dipoles calculated using eq 2.

DPPC reorient with a decay time of τ = 12.7 ns, whereas the unbound decay time is τ = 1.0 ns.

On the basis of these results for the orientation and dynamics of the molecular dipoles, we conclude that the TR−DHPE−DPPC binding is largely due to electrostatic interactions, the largest being charge−dipole and dipole−dipole. We cannot rule out the possibility of entropic contributions to the binding energy. The highly charged sulfonate and sulfonyl groups of Texas Red force the aromatic, aryl ring well into the polar interphase[27] which may favor being flanked by a DPPC headgroup over solvation by water. There also may be a steric contribution to the binding; it has been pointed out, e.g., that the behavior of charged lipids such as POPA can only be explained as a combination of electrostatic and steric effects.[34]

Impact of Texas Red on Bilayer Dynamics. Fluorescence labeling is often used to probe the dynamics of lipid bilayer systems. For example, a variety of fluorescence techniques, such as FRAP, FCS, and SMT, are employed to determine diffusion coefficients in lipid membranes.[35] In all of these cases, the experiment is probing the diffusion coefficient of the fluorescent molecule, and not the tracer diffusion of the unlabeled lipids.

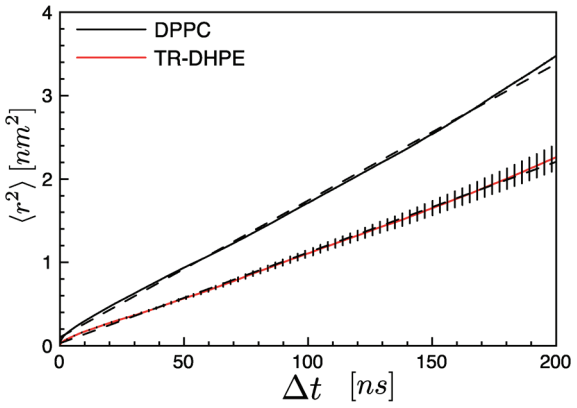

Figure 8. Lateral mean square displacement of DPPC phosphorus atoms and TR−DHPE aromatic oxygens in the 24-TR system. Dashed lines are least-squares fits to eq 3, but allow for a nonzero intercept to account for the nonlinearity at small times. Measured values for the diffusion coefficients are D_{DPPC} = 4.1 μm^2/s and $D_{\mathrm{TR-DHPE}}$ = 2.7 μm^2/s. The larger error bars for TR−DHPE are due to the fact that there are 24 molecules in the ensemble average, versus 488 for the DPPC.

Therefore, it must be assumed that the fluorescent molecule mimics the behavior of the unlabeled molecules of interest. This assumption deserves careful consideration, especially given that many fluorescent molecules possess a net charge and are nearly as massive as the molecules they are attached to.

To compare the diffusion coefficient of unlabeled DPPC molecules to its fluorescent analogue TR−DHPE, we used a mean square displacement (MSD) analysis. For a normally diffusing particle, the diffusion coefficient D is the proportionality constant between the mean square displacement and the time lag Δt. For a two-dimensional system, like a lipid bilayer, there is an additional factor of 4,

$$\langle r^2(\Delta t) \rangle = 4D\Delta t \tag{3}$$

The time lag Δt is a sliding time window over the trajectory and the mean is an ensemble average. Presented in Figure 8 is the mean square displacement of DPPC phosphorus atoms and the aromatic oxygens of TR−DHPE. Although at short times, different atoms of a molecule will have different MSD behavior, they will converge to the molecular MSD for $\Delta t \gtrsim 10$ ns.[36] We chose the aromatic oxygen of TR−DHPE because it is near the center of the excitation dipole of Texas Red, which is the origin of the fluorescent signal measured experimentally.

Using a least-squares fit of eq eq 3 to the MSDs of Figure 8, and allowing for a nonzero intercept, we find that the TR−DHPE diffusion coefficient, $D_{\mathrm{TR-DHPE}}$ = 2.7 μm^2/s, is 34% lower than the DPPC diffusion coefficient, D_{DPPC} = 4.1 μm^2/s. This reduction in the diffusion coefficient can be understood in light of the Texas Red - DPPC binding and the size dependence of diffusion in a lipid bilayer. The tracer diffusion of lipids is quantitatively described by the free-area model,[37] but the diffusion of particles with an in-plane area >1 nm^2 seems to be well described by the continuum theory of Saffman and Delbrück,[38] which predicts a $\ln(1/R)$ dependence on the particle's radius. Several experiments[39,40] and simulations[41] have demonstrated the suitability of these models and a cross over from free-area type behavior to $\ln(1/R)$ behavior at $a \sim 1$ nm^2. As TR−DHPE and DPPC have identical acyl chains, the bound species has about four acyl chains and can be thought of as Texas Red

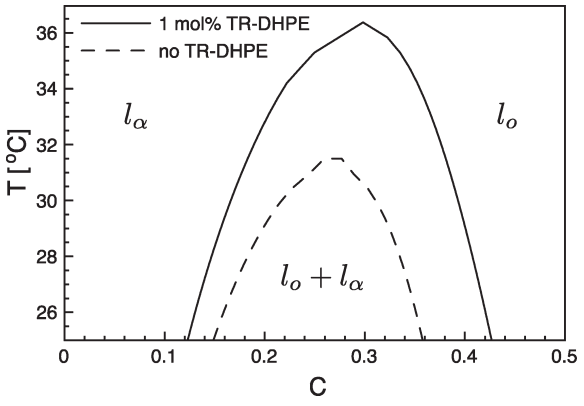

Figure 9. Estimated change in phase behavior of a hypothetical ternary lipid system upon addition of 1 mol % TR−DHPE. The lower axis is the mol fraction of cholesterol. The ternary system consists of 40 mol % saturated lipid (s), 1 mol % TR−DHPE (z), each of which has bound 1.2 unsaturated lipids, the indicated concentration of cholesterol (c) and unsaturated lipid (u), such that $s + z + c + u = 1$. The temperature axis was scaled to fit the no TR−DHPE phase boundary to experimental phase diagrams[46] and is only approximate.

binding together two phospholipids. If we assume a DPPC area per lipid of $a \sim 0.66$ nm^2, the bound species has an approximate area of $a \sim 1.32$ nm^2, or slightly more due to the Texas Red.[27] This puts DPPC and the TR−DHPE bound species on either side of the $a \sim 1$ nm^2 discontinuity, yet we find good agreement with the results of Liu et al., who studied the size dependent diffusion coefficient of amphiphilic molecules with varying numbers of acyl chains.[42] They found that the four acyl chain species had a diffusion coefficient 21%−35% lower than the two acyl chain species, depending on temperature.[42] We therefore conclude that the lower Texas Red diffusion coefficient is due to the TR−DHPE binding a DPPC molecule. This might not always be a problem experimentally. For example, if the relative change in diffusion coefficient is being measured with respect to a change in viscosity, the results would be unchanged. However, any change that might alter the TR−DHPE−DPPC binding equilibrium, such as temperature, would affect the underlying Texas Red diffusion coefficient.

Impact of Texas Red on Bilayer Phase Behavior. TR−DHPE - DPPC binding is expected to have a significant impact on the phase behavior of the lipid bilayer. A recent thermodynamic model showed that by cross-linking lipids in a ternary lipid system, the region of phase coexistence was expanded.[43,44] This result derives from the lower mixing entropy of the system with cross-linked lipids. The model was developed to help explain observations of phase separation being promoted by cross-linking plasma membrane components. Our system can be thought of as Texas Red binding, or cross-linking, two lipids so we would expect a change in phase behavior for a ternary lipid system containing TR−DHPE. This is significant because TR−DHPE is often used experimentally to study phase behavior of ternary (unsaturated, saturated and cholesterol) lipid systems.[45]

To make predictions about the impact of TR−DHPE on bilayer phase behavior, we used the theory of Putzel et al. to plot the phase diagram for a hypothetical lipid membrane, with and without Texas Red (Figure 9). The basic model is a mixture of four components: saturated lipids (s), unsaturated lipids (u), cholesterol (c), and some concentration (z) of saturated or unsaturated lipids bound into clusters of p molecules[43] We determined that TR−DHPE binds to an average of 1.2 lipid molecules (see Figure 3 (inset)), so to model the inclusion of 1 mol % TR−DHPE, we set $p = 2.2$ (counting the lipid portion of TR−DHPE) and $z = 0.02$. We assume that TR−DHPE binds to the unsaturated lipid because TR−DHPE partitions into the unsaturated lipid, disordered phase, although the results would be qualitatively the same if it were bound to the saturated component.[43] In order to show the temperature dependence, we hold the saturated component constant $s = 0.4$ and vary the cholesterol concentration, c. The model[44] contains Flory−Huggins type interaction parameters which are inversely proportional to temperature, so the variation in temperature in the phase diagram is brought about by changing the interaction parameters.

Qualitatively, we see that the addition of 1 mol % TR−DHPE increases the critical temperature. We also find that the critical cholesterol concentration increases about 20%. If TR−DHPE bound the saturated lipid, the critical temperature would still increase, but the critical cholesterol concentration would decrease, due to the attractive saturated-cholesterol interaction in the model. To be more quantitative about the increase in critical temperature, we estimated a temperature scale based on a phase diagram derived from NMR experiments.[46] By fitting the no TR−DHPE phase diagram to the NMR phase diagram,[46] we find that the addition of 1 mol % TR−DHPE increases the critical temperature on the order of 5 °C.

An increase in mixing transition temperature is consistent with a number of experimental reports. Juhasz et al. systematically investigated the mixing transition temperature (T_{mix}) in giant unilamellar vesicles with a variety of fluorescent probes.[6] Unfortunately for us, TR−DHPE was used as the reference, but still some probes, including rhodamine−DHPE, were found to increase T_{mix} by 3−4 °C. Of all the lipid analogue probes studied, only one, Bodipy−PC, was neutral and it was the only probe to produce a T_{mix} value lower than TR−DHPE. In 2007, Veatch et al. used NMR to show that very small concentrations of the probes DiI and DiO (~0.2 mol %), both of which are charged, increased T_{mix} by 5 °C.[5]

TR−DHPE was also used in a series of studies that used fluorescence microscopy in parallel with NMR to investigate the phase behavior of DOPC/DPPC/cholesterol mixtures.[45−47] The increase in T_{mix} that we predict should have been observed in each of these studies. In fact, differences in behavior were observed between the fluorescence and NMR experiments that were consistent with our prediction, but the changes were attributed to affects other than fluorescent labeling. For example, Veatch et al. observed large scale phase separation ($d \gg 160$ nm) at higher temperatures when using TR−DHPE compared to NMR experiments which used no TR−DHPE.[45] They interpreted the lower NMR transition as something called T_{low} and identified the onset of small composition fluctuations ($d \ll 160$ nm) as corresponding to the large scale phase separation seen with TR−DHPE (T_{mix}). Davis et al. interpreted their results in a similar way.[46] For a composition of 35:35:30 DOPC/DPPC/cholesterol, phase separation on a scale greater than ~250 nm occurred at 26 °C, but T_{mix} was said to be ~30 °C where there were small composition fluctuations which were not observed using fluorescence. Juhasz et al. observed a 3−4 °C increase in T_{mix} with TR−DHPE compared to NMR, but they attributed the difference to the deuterium labeling reducing T_{mix} in the NMR experiments.[47] However, when comparing TR−DHPE labeled vesicles with deuterated or nondeuterated lipids, there only seems to be a ~2 °C change in T_{mix}. One way to experimentally

determine whether TR−DHPE increases T_{mix}, would be to use NMR on samples with and without TR−DHPE.

CONCLUSION

We conducted a 500 ns, atomistic simulation of a TR−DHPE labeled DPPC bilayer to determine what influence Texas Red labeling has on a lipid bilayer. The most significant finding, and one that has further implications, was the binding between TR−DHPE and DPPC. We found that TR−DHPE is on average, bound to 1.2 DPPC molecules. A subsequent change in orientation and dynamics of the bound DPPC dipoles indicated that binding is caused by charge-dipole and dipole−dipole interactions between TR−DHPE and DPPC. Binding changes the dynamics and phase behavior of the lipid bilayer. We found that TR−DHPE has a diffusion coefficient ∼30% lower than DPPC which is consistent with the idea of the TR−DHPE bound entity being about the size of two DPPC lipids. We also estimate that binding would increase the mixing transition temperature of a ternary lipid system by about 5 °C. Interestingly in bilayer mixtures of phospholipids with PEO attached phospholipids there is a complex formation which starts at roughly the same concentration.[48] Our results indicate that even small concentrations of fluorescent probes, especially when strong electrostatic interactions are present, can have a significant impact on the properties of a lipid bilayer. It is therefore important in experiments to at least briefly consider whether the fluorescent probe might change the results in a way that would alter the conclusions. However, one also has to be aware that most experiments are performed at lower temperatures than the ones considered here (325 K).

AUTHOR INFORMATION

Corresponding Author

*E-mail: rfaller@ucdavis.edu.

ACKNOWLEDGMENT

Financial Support from the Graduate Assistance in Areas of National Need (GAANN) Program of the US Department of Education and Grant CBET 05066602 from the US National Science Foundation is gratefully acknowledged.

REFERENCES

(1) Baumgart, T.; Hess, S. T.; Webb, W. W. *Nature* **2003**, *425*, 821–824.
(2) Schwille, P.; Korlach, J.; Webb, W. *Cytometry* **1999**, *36*, 176–182.
(3) de Almeida, R.; Loura, L.; Fedorov, A.; Prieto, M. *J. Mol. Biol.* **2005**, *346*, 1109–1120.
(4) Schutz, G. J.; Sonnleitner, M.; Hinterdorfer, P.; Schindler, H. *Mol. Membr. Biol.* **2000**, *17*, 17–29.
(5) Veatch, S. L.; Leung, S. S. W.; Hancock, R. E. W.; Thewalt, J. L. *J. Phys. Chem. B* **2007**, *111*, 502–504.
(6) Juhasz, J.; Davis, J.; Sharom, F. *Biochem. J.* **2010**, *430*, 415–423.
(7) Bouvrais, H.; Pott, T.; Bagatolli, L.; Ipsen, J.; Méléard, P. *Biochim. Biophys. Acta, Biomembr.* **2010**, *1738*, 1333–1337.
(8) Daniel, S.; Diaz, A.; Martinez, K.; Bench, B.; Albertorio, F.; Cremer, P. *J. Am. Chem. Soc.* **2007**, *129*, 8072–8072.
(9) Groves, J. T.; Ulman, N.; Boxer, S. G. *Science* **1997**, *275*, 651–653.
(10) Brozell, A.; Muha, M.; Sanii, B.; Parikh, A. *J. Am. Chem. Soc.* **2006**, *128*, 62–63.
(11) Veatch, S. L.; Keller, S. L. *Biochim. Biophys. Acta* **2005**, *1746*, 172–185.
(12) Titus, J.; Haugland, R.; Sharrow, S.; Segal, D. *J. Immunol. Methods* **1982**, *50*, 193–204.
(13) Baumgart, T.; Hunt, G.; Farkas, E. R.; Webb, W. W.; Feigenson, G. W. *Biochim. Biophys. Acta, Biomembr.* **2007**, *1768*, 2182–2194.
(14) Cascales, J.J. L.; Huertas, M.; de la Torre, J. G. *Biophys. Chem.* **1997**, *69*, 1–8.
(15) Repáková, J.; Čapková, P.; Holopainen, J. M.; Vattulainen, I. *J. Phys. Chem. B* **2004**, *108*, 13438–13448.
(16) Repáková, J.; Holopainen, J. M.; Morrow, M. R.; McDonald, M. C.; Čapková, P.; Vattulainen, I. *Biophys. J.* **2005**, *88*, 3398–3410.
(17) Hoff, B.; Strandberg, E.; Ulrich, A. S.; Tieleman, D.; Posten, C. *Biophys. J.* **2005**, *88*, 1818–1827.
(18) Čurdová, J.; Čapková, P.; Plášek, J.; Repáková, J.; Vattulainen, I. *J. Phys. Chem. B* **2007**, *111*, 3640–3650.
(19) Loura, L. M.; Ramalho, J. P. *Biochim. Biophys. Acta* **2007**, *1768*, 467–478.
(20) Loura, L. M.; Fernandes, F.; Fernandes, A.; Ramalho, J. P. *Biochim. Biophys. Acta, Biomembr.* **2008**, *1778*, 491–501.
(21) Repáková, J.; Holopainen, J. M.; Karttunen, M.; Vattulainen, I. *J. Phys. Chem. B* **2006**, *110*, 15403–15410.
(22) Gullapalli, R.; Demirel, M.; Butler, P. *Phys. Chem. Chem. Phys.* **2008**, *10*, 3548–3560.
(23) Lindahl, E.; Hess, B.; van der Spoel, D. *J. Mol. Model* **2001**, *7*, 306–317.
(24) Berendsen, H. J. C.; van der Spoel, D.; van Drunen, R. *Comput. Phys. Commun.* **1995**, *91*, 43–56.
(25) van der Spoel, D.; Lindahl, E.; Hess, B.; Groenhof, G.; Mark, A.; Berendsen, H. J. C. *J. Comput. Chem.* **2005**, *26*, 1701.
(26) Berger, O.; Edholm, O.; Jahnig, F. *Biophys. J.* **1997**, *72*, 2002–2013.
(27) Skaug, M.; Longo, M. L.; Faller, R. *J. Phys. Chem. B* **2009**, *113*, 8758–8766.
(28) Berendsen, H. J. C.; Postma, J. P. M.; van Gunsteren, W. F.; Hermans, J. In *Intermolecular Forces*; Pullman, B., Ed.; D. Reidel Publishing Company: Dordrecht, The Netherlands, 1981; Chapter Interaction models for water in relation to protein hydration, pp 331−342.
(29) van Gunsteren, W. F.; Berendsen, H. J. C. *Groningen Molecular Simulation (GROMOS) Library Manual*; BIOMOS b.v.: Groningen, The Netherlands, 1987.
(30) Berendsen, H. J. C.; Postma, J.; van Gunsteren, W.; DiNola, A.; Haak, J. *J. Chem. Phys.* **1984**, *81*, 3684–3690.
(31) Hess, B.; Bekker, H.; Berendsen, H. J. C.; Fraaije, J. *J. Comput. Chem.* **1997**, *18*, 1463–1472.
(32) Miyamoto, S.; Kollman, P. *J. Comput. Chem.* **1992**, *13*, 952–962.
(33) Essmann, U.; Perera, L.; Berkowitz, M.; Darden, T.; Lee, H.; Pedersen, L. *J. Chem. Phys.* **1995**, *103*, 8577.
(34) Dickey, A. N.; Faller, R. *Biophys. J.* **2008**, *95*, 2636–2646.
(35) Guo, L.; Har, J. Y.; Sankaran, J.; Hong, Y.; Kannan, B.; Wohland, T. *ChemPhysChem.* **2008**, *9*, 721–728.
(36) Wohlert, J.; Edholm, O. *J. Chem. Phys.* **2006**, *125*, 204703.
(37) Vaz, W. L. C.; Clegg, R. M.; Hallmann, D. *Biochemistry* **1985**, *24*, 781–786.
(38) Saffman, P. G.; Delbruck, M. *Proc. Natl. Acad. Sci. U. S. A.* **1975**, *72*, 3111–3113.
(39) Ramadurai, S.; Holt, A.; Krasnikov, V.; van den Bogaart, G.; Killian, J.; Poolman, B. *J. Am. Chem. Soc.* **2009**, *131*, 12650–12656.
(40) Lee, C.; Petersen, N. *Biophys. J.* **2003**, *84*, 1756–1764.
(41) Guigas, G.; Weiss, M. *Biophys. J.* **2006**, *91*, 2393–2398.
(42) Liu, C.; Paprica, A.; Petersen, N. *Biophys. J.* **1997**, *73*, 2580–2587.
(43) Putzel, G. G.; Schick, M. *Biophys. J.* **2009**, *96*, 4935–4940.
(44) Putzel, G. G.; Schick, M. *Biophys. J.* **2008**, *95*, 4756–4762.
(45) Veatch, S. L.; Polozov, I. J.; Gawrisch, K.; Keller, S. L. *Biophys. J.* **2004**, *86*, 2910–2922.
(46) Davis, J.; Clair, J.; Juhasz, J. *Biophys. J.* **2009**, *96*, 521–539.
(47) Juhasz, J.; Sharom, F.; Davis, J. *Biochim. Biophys. Acta, Biomembr.* **2009**, *1788*, 2541–2552.
(48) Lozano, M. M.; Longo, M. L. *Soft Matter* **2009**, *5*, 1822–1834.